Chapter 9

Polymer Nanocomposite Artificial Joints

Samy Yousef

Additional information is available at the end of the chapter

http://dx.doi.org/10.5772/62269

Abstract

Artificial joints (AJ) often have a polymeric component to decrease the wear rate and the total weight at the same time and make it more flexible. Ultrahigh molecular weight polyethylene (UHMWPE) is considered as the standard material for these applications. Therefore, UHMWPE has been reinforced by many of the nanomaterials, hoping to improve the tribology characteristic, which is considered as the most important factor in determining the life span of AJ. However, all attempts were in laboratory scale and did not live up to the actual implementation due to the high viscosity of UHMWPE, leading to poor dispersion with bulk components. This chapter aims to explain in detail a novel technique to produce a real UHMWPE nanocomposite (UNC) hip cup using the paraffin oil dispersion technique and tested by an artificial joint simulator (AJS), which was designed by the author. The chapter contains three parts: the first part starts with a brief account of AJ and then illustrates the AJ polymeric components. The wear behavior of the polymeric components is also presented. The second part reviews some previous attempts for the synthesis of UNC and the common nanomaterials [carbon nanofiber (CNF), carbon nanotubes (CNT), and graphene (GA)], which are used as a nanofiller. The problems that had arisen during the mixing process and UNC characterizations are also presented. For the third part, the chapter concludes by explaining a novel technique to produce UHMWPE hip cup reinforced by CNT using the paraffin oil dispersion technique and testing by AJS, which was designed especially for this.

Keywords: artificial joint simulator, artificial joints, carbon nanofiber, carbon nanotubes, graphene, paraffin oil dispersion technique, polymer nanocomposites, polymer nanocomposite hip cup, UHMWPE, wear

1. Artificial joints (AJ)

1.1. Introduction

The human body contains many orthopedic joints to give it more flexibility during movement (**Figure 1**). Usually, the damages in these joints occur due to internal effects and environmental changes, such as weather and pollution, in addition to bad nutrition and especially calcium deficiency, as well as advancing age and the diseases of aging. However, the possibility of damage is significant in the hip, shoulder, knee, and fingers as a result of exposure to overload. Currently, millions of orthopedic patients around the world are suffering from pain and psychological disorders, even after performing joint replacement procedures, due to the short life span for the AJ, and this means the return of pain from thus restoring the implant and additionally the extra cost of the implant [2]. To eliminate pain, increase mobility, and restore the quality of life, AJ was innovated in 1961 when Sir John Charnley performed the procedure of the first surgery to implant joint prostheses successfully in a particular artificial hip joint [3]. At the time, AJ was proven to be an extremely successful and cost-effective means of relieving arthritis pain. After that, AJ has been extended to include shoulder, knee, and finger joint replacement bearings. **Figure 2** shows the AJ radiographs for the hip, shoulder, knee, and finger joint bearings respectively [4–7]. This section presents the AJ components and the common methods used to investigate the wear behavior for AJ polymeric components and its failure shapes.

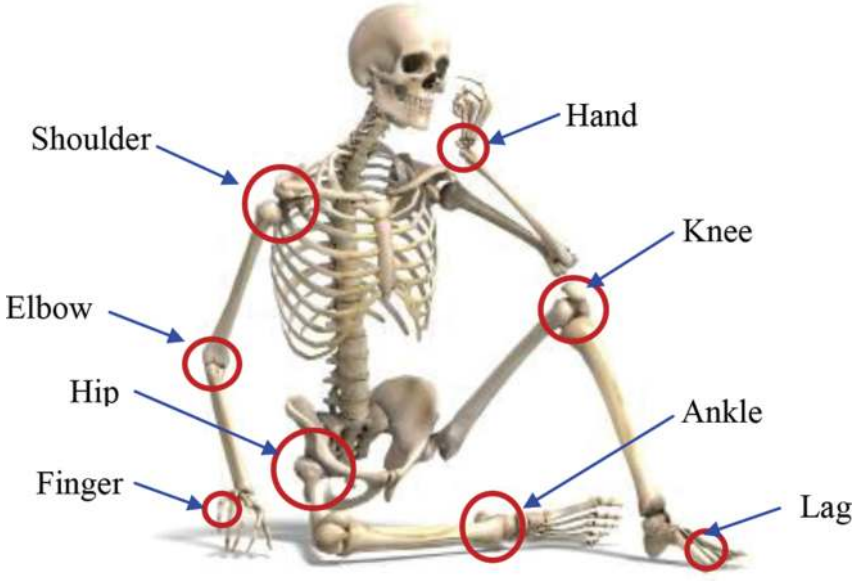

Figure 1. Schematic drawing for human body joints [1].

http://dx.doi.org/10.5772/62269

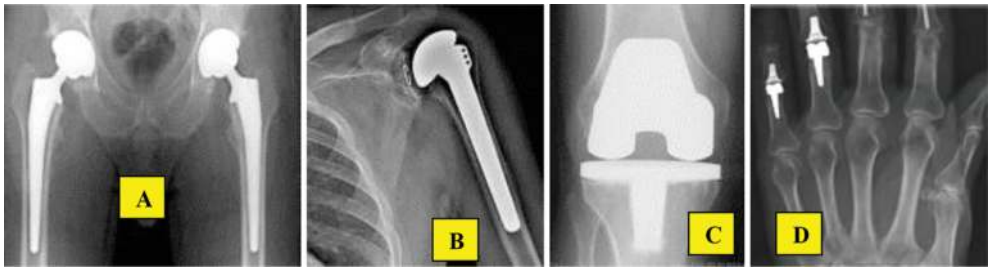

Figure 2. AJ radiographs of (A) hip, (B) shoulder, (C) knee, and (D) finger joints.

1.2. AJ components

The hip, shoulder, knee, and finger AJ prostheses are usually composed of two main components articulating with one another, polymeric against a metal or ceramic component (**Figure 3**). This section focuses on the polymeric material components that consider the weaker part in total AJ components. At the beginning, polytetrafluoroethylene (PTEF) and polyaryletheretherketone (PEEK) polymeric materials have been employed in these applications, but the results were not good due to the large aseptic loosening and osteolysis [8]. Nonetheless, ultrahigh molecular weight polyethylene (UHMWPE) remains the gold standard polymeric material for AJ component due to its many unique properties, such as high wear resistance, strength, modulus, excellent toughness, chemical resistance and impact, low moisture absorption, good wave transmission, and electrical insulation [9]. In addition, the mechanical and wear properties of UHMWPE are considered the most important effective factors, which can be controlled at the service time of the total joint [10].

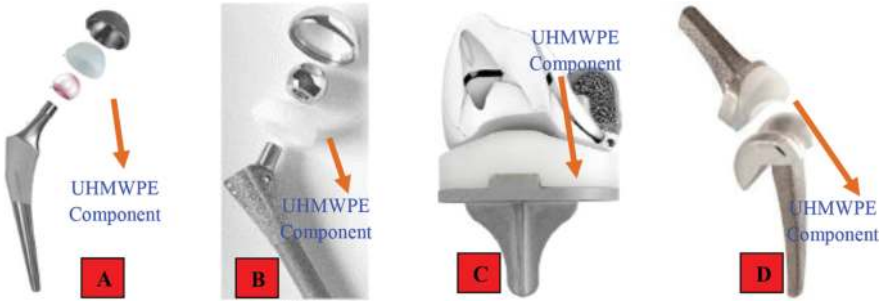

Figure 3. Contemporary AJ prosthesis system components for (A) hip, (B) shoulder, (C) knee, and (D) finger bearing joints [11].

1.3. Investigation of AJ polymeric component wear

In general, the UHMWPE components in the AJ are considered the weaker components, and failure happens due to two kinds of wear failure [sliding and rolling (abrasive and adhesive)] as a result of sliding between polymeric and metal components [12]. The established wear depends on several variables such as load (pressure), speed, contact geometry, state of lubrication, and roughness [13]. Nevertheless, it is difficult to take all these variables into consideration. The pin-on-disc or ball-on-disc machine is considered the leading method to evaluate the wear behavior (in the form of weight loss or volume loss) under constant load conditions [14]. To increase the accuracy of wear investigation and to simulate the real failure condition, many previous test rigs or joint replacement simulators (JRS) have been designed and built to measure the wear rate of hip, shoulder, and finger joint bearings under different conditions. The basic difference between each JRS and another is the loading mechanism (**Figure 4**).

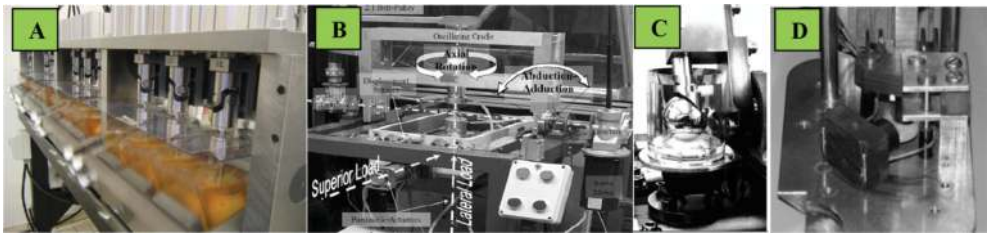

Figure 4. AJ wear simulators of (A) hip, (B) shoulder, (C) knee, and (D) finer joints [15–18].

1.4. Failure of AJ polymeric components

Studies that were conducted on the failure of polymeric components in AJ point to the damages that were featured in the following forms: rim erosion, surface irregularities, component fracture, and wear [19]. Wear failure is considered a key design parameter of AJ and the created wear particles might be the reason for component loosening, leading to pain and the need for

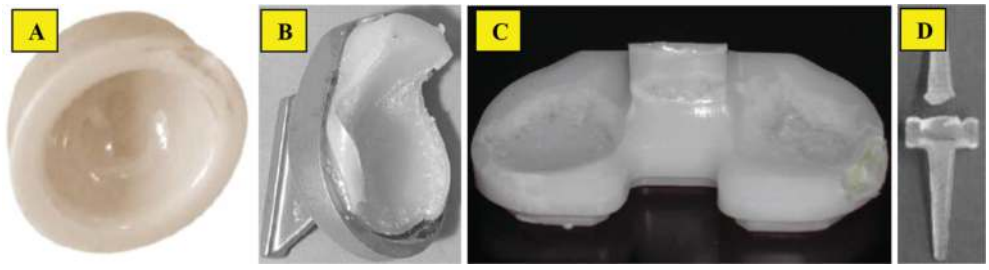

Figure 5. Photograph of failure shapes of (a) hip, (b) shoulder, (c) knee, and (d) finger polymeric components [18–21].

a revision operation [20]. **Figure 5** shows the photograph failure of the polymeric components of the hip, shoulder, knee, and finger, respectively. It is clear that the main failure is located on the contact surface between femoral (metal component) and tested (UHMWPE component) samples. Also, it has seen that failure occurs due to three reasons: scratching, pitting, and delamination or cracking [21].

2. Nanocomposite polymer biomaterials

2.1. Introduction

With the increasing demand for AJ, it has become necessary to improve the mechanical and wear behaviors of UHMWPE component to increase the total life span of joints and also to keep pace with the progress for prosthetic applications. Nanotechnology science is considered the most appropriate alternative at the moment after it that has proven high efficiency in many areas, especially in polymer nanocomposites. Mixing UHMWPE with nanofiller materials, which have a higher surface area to volume ratio, leads to rapid interaction and more mixing between the nanofiller and UHMWPE and thus improvement of the chemical and physical properties [22]. This section reviews the common nanofiller materials, which are used to improve the properties of UHMWPE. In addition, different dispersion methods were used to obtain a uniform dispersion. Finally, the characterization methods for the synthesized UHMWPE nanocomposite (UNC) have been listed.

2.2. Nanofiller materials

There are many types of nanofiller materials that have a good tribological characteristic reinforced by UHMWPE such as carbon nanofibers (CNF), carbon nanotubes (CNT), and graphene (GA) for the synthesis of UNC to have a good wear resistance [23–25]. The results showed that GA and CNT additives have been proven more effective compared to other nanofillers because GA and CNT have unique physical, mechanical, tribological, high aspect ratio, and chemical properties. Also, GA has better biocompatibility compared to other nanofiller materials [25]. Although CNT is widely used, it has to be economic. This chapter focuses on the CNT/UHMWPE synthesis. Therefore, this study focuses on CNT as an economic nanofiller material. CNT is composed of molecular-scale sheets of graphite called GA that roll up to make a tube. CNT can be classified into single-wall nanotubes (SWCNT) and multiwall nanotubes (MWCNT). SWCNT consists of single GA rolls, whereas MWCNT consists of two or more coaxial tubes within a tube [26]. There are three common different methods used for the synthesis of CNT: arc discharge, laser vaporization, and chemical vapor deposition (CVD) [27]. Arc discharge multielectrode and CVD multiquartz tubes were designed and built to produce CNT with high yield and that is more economic (**Figure 6**). Finally, **Figure 7** illustrates the different carbon structures between single-wall and multiwall CNT using transmission electron microscopy (TEM).

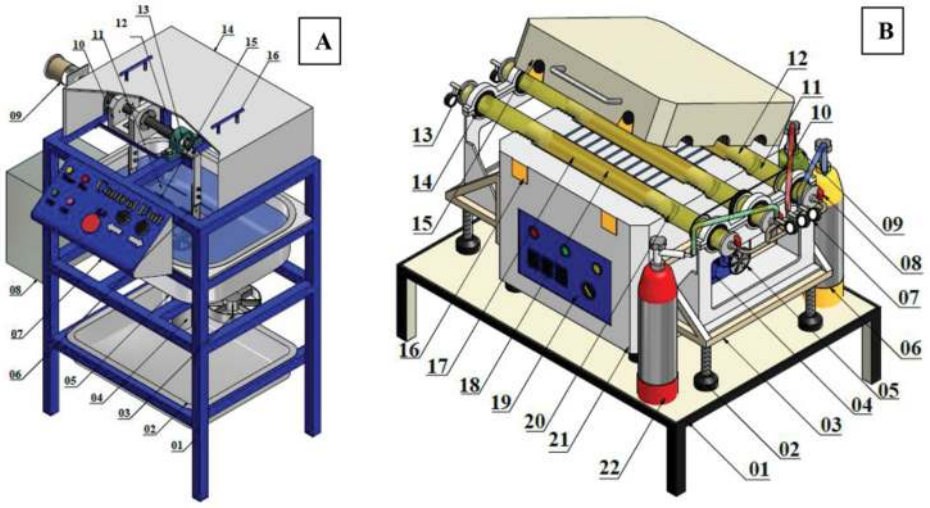

(A) Arc discharge multi-electrodes technique
(1) Base frame, (2) lower tank, (3) fans for cooling, (4) valve, (5) upper tank, (6) carbon holder, (7) control unit, (8) electrical unit, (9) steeper motor, (10) nuts housing, (11) deionized water, (12) power screw, (13) bearing, (14) cover, (15) pure graphite, (16) cover hand.
(B) CVD multi-quartz tubes technique
(1) Base, (2) Set screw, (3) Bearing holder, (4) Motor, (5) Sprocket, (6) Argon cylinder, (7) Pressure gauge, (8) Control valve, (9) Hydrogen cylinder, (10) Chain, (11) Quartz tube, (12) Ceramic sealant, (13) Exhaust gas, (14) Bearing, (15) Furnace movable part, (16) Padlock, (17) Heater, (18) Catalyst position, (19) Control unit, (20) Graphite rings, (21) Furnace fixed part, (22) Methane cylinder.

Figure 6. Fully automatic system for producing CNT using arc discharge multielectrode CVD multiquartz tube design [28,29].

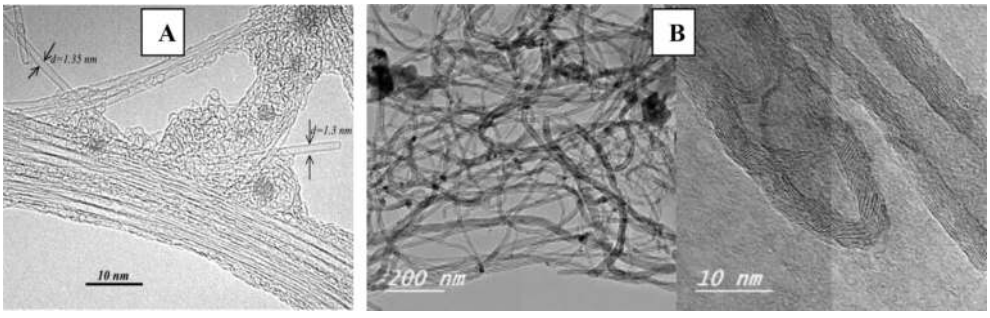

Figure 7. TEM images of (A) SWCNT and (B) MWCNT [29,30].

http://dx.doi.org/10.5772/62269

2.3. Dispersion of UNC polymer

In the dispersion system, UHMWPE and nanofiller particle materials are dispersed in a continuous phase with a different composition. Several methods of mixing techniques were employed to prepare UHNs, such as (a) hot plate and magnetic stir bar, (b) ultrasonic bath, (c) ball milling, (d) twin-screw extrusion, and (e) three roll mill. It is worth mentioning that each technique has different mixing conditions to improve the dispersion of nanofiller inside UHMWPE polymer base. Most mixing conditions are focused on the mixing temperature and mixing time. **Figure 8** shows the dispersion techniques with different mixing parameters. Finally, all the previous dispersion methods obtain UHNs in powder shape expected Min-Lab Extruder given in wire form and then cut into small pieces (pellets), as shown in **Figure 9**.

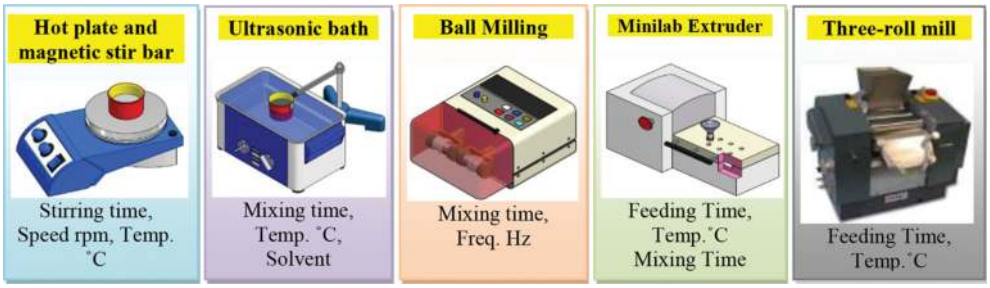

Figure 8. Nanocomposite UHMWPE dispersion [31].

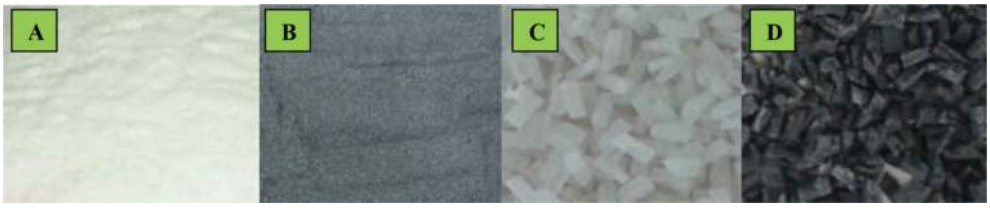

Figure 9. Compression conditions and hot press components [32].

2.4. Synthesis of UNC polymer

To produce the final sheet or film, hot press can be employed to compress the powder or pellet UNC inside copper or aluminum die between two Teflon sheets to produce UNC sheets with very fine surfaces and uniform thickness as shown in **Figure 10**. It is worth mentioning that each type of polymeric material has different compression conditions depending on the melting temperature and viscosity. This section focuses on UHMWPE compression conditions. UNC can be found in two forms: powder or pellets. The powder shape can be produced by magnetic stirring, ultrasonic bath, ball milling, and three roll mill, whereas the pellet shape

can be produced by twin-screw extrusion. **Table 1** shows the compression conditions of UNC in powder and pellet shapes at 200°C and a pressure of 200 bar.

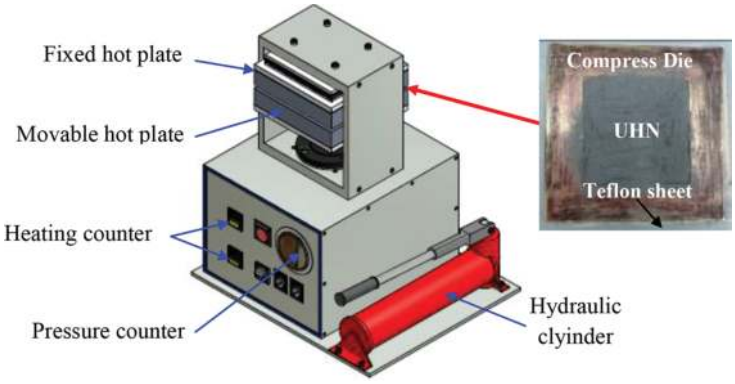

Figure 10. Hot press schematic drawing.

	Powder		Pellets	
Step. no.	Time (min)	Pressure (bar)	Time (min)	Pressure (bar)
1	1	0	10	Without pressure
2	1	50	5	0
3	1	100	4	50
4	1	150	4	100
5	16	200	4	150
6			16	200

Table 1. Compression conditions of UNC [31,32]

2.5. UNC polymer characterizations

After preparing the UNC sheets using the previous steps, the following procedures were used to study the effect of nanofiller adding on UHMWPE characterizations. In this section, the author shows the effect of the feeding ratio of the CNT on the different properties of UHMWPE. Also, other nanofiller additives such as GA and CNF are presented just for comparison.

2.5.1. Scanning electron microscopy (SEM)

SEM was used to examine the dispersion of nanofillers inside UHMWPE. **Figure 11** shows the fracture surfaces of virgin UHMWPE and UHMWPE reinforced by GA, CNT, and CNF. As

clearly seen from the SEM images, the incorporation of CNT, GA, and CNF in the UHMWPE matrix resulted in a drastic change in the topography of the fracture surfaces, whereas the fracture surfaces of virgin UHMWPE are smoother.

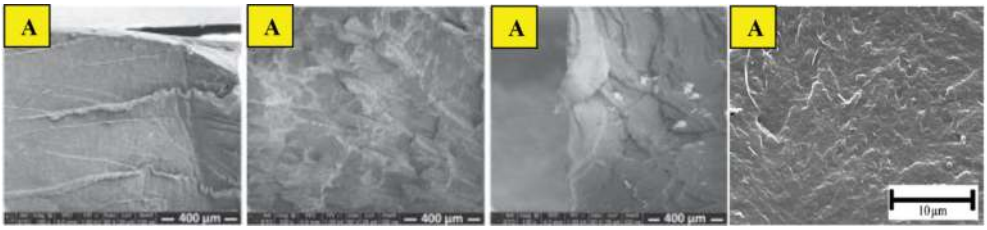

Figure 11. SEM images of fracture surface of (A) UHMWPE, (B) GA/UHMWPE, (C) CNT/UHMWPE, and (d) CNF/UHMWPE [24,33].

2.5.2. Differential scanning calorimetry (DSC)

DSC was used to investigate the thermal properties (crystallization temperature, melting temperature, and lamellar thickness) of UNC. The tests were carried out in nitrogen ambient environment with a heating rate of 10°C/min until 230°C, and then the specimen cools down to room temperature with cold water [34]. The previous results showed that the melting temperature and crystallinity degree increased by adding nanofiller, whereas the lamellar thickness was decreased. This indicated that CNT acted as effective heterogeneous nucleating agents to facilitate the crystallization of UHMWPE [35].

2.5.3. Rheological performance of GUC

UHMWPE has high viscosity (η) representing the main obstacle for blends with the nanofiller materials; more precisely, high η means bad dispersion [36]. The parallel plate rheometry was used to investigate the rheological properties of UNC, particularly viscosity and elastic modulus. The tested samples were cut according to ASTM standard into round shapes having a diameter of 25 mm and thickness of 1 mm. The tests conducted with following data gape 1 mm at stress-controlled rheometer in constant strain mode. The experiment was performed in the linear viscoelastic regime at a temperature up to 180°C and frequency range from 0.005 to 100 Hz and the applied strain was controlled at 0.5% [37]. Unfortunately, all the previous results showed that the viscosity of UHMWPE was increased by the addition of a nanofiller and this led to bad dispersion [38]. To avoid this problem, Galetz et al. and Wood et al. used PO as a solvent and assisted melt material during the mixing process, respectively, and then extracted PO to decrease η of UHMWPE; the result was uniform dispersion approximately [24].

2.5.4. Mechanical properties

The manual press was used to prepare the standard tensile specimens according to ASTM D638-10 standard or any standard. The mechanical properties of UNC standard specimens can

be measured by universal testing machine with load cell of 500 N and crosshead speed of 10 mm/min. The results showed that the addition of nanofiller leads to significant improvement in the mechanical properties with varying proportions, and the variance depends on the percentage weight of the filler and dispersion technique. In general, the mechanical properties of UHMWPE improved due to the increase of the crystallinity degree [39].

2.5.5. Wear behaviors

JRS are still not widely used to test UNC components due to economic reasons, especially as the shape of the testing samples is more complicated. The pin-on-disk or ball-on-disk test rig is recommended in these applications to overcome the previous problems (**Figure 12**). In this case, the tested UNC sample may be flat or cylindrical shape sliding against stainless steel or ceramic pin. The specific wear rate in this case depends on four parameters: applied normal load, speed, test duration, and type of lubricant. Furthermore, the specific wear rate can be calculated by the following equation.

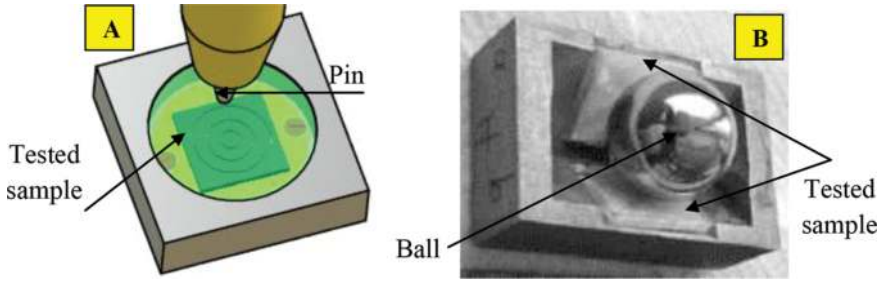

Figure 12. (A) Pin-on-disc test rig model and (B) ball-on-disc model [14,35].

The previous results showed that the wear resistance of UHMWPE has been improved by adding a nanofiller, especially CNT and GA, because CNT and GA have a high aspect ratio. Also, the addition of CNT and GA leads to increase the melting temperature, which considers the obstacle in wear progress [35]. The wear particles are created due to the continuous sliding between UNC and the stainless steel pin, as thermal softening and the melting of the surface layer materials occurred. The surface layer increases over time and causes several scratches inside the wear track. In addition, the wear mechanism can be found in two forms: ductile or brittle fractures. The brittle fracture is safer when compared to ductile fracture, because the amount of materials removed in the form of particles is less.

$$Ws = \frac{\Delta m}{\mathcal{P}\, x\, Fn\, x\, L}$$

Where W_s (10^{-6}mm^3/Nm) is the specific wear rate, Δm (mg) is the mass loss of the specimen and measured by using a high sensitivity electronic weighing balance with accuracy

(10^{-4}gram), p (g/ml) is the density of the specimen, F_n (N) is the normal load and L *(m)* is the total sliding distance.

Finally, **Figure 13** shows the three wear mechanisms of UHMWPE reinforced by CNF, CNT, and GA. It is clear that the amount and length of the removed chips decrease with the addition of CNF (as indicated in the images by circles). While adding CNT and GA, the removed chips are converted to discontinuous chips or small particles, especially with GA, due to the high aspect ratio of GA. Well-dispersed GA in UHMWPE provided a large surface area available for the interaction between UHMWPE molecules and GA, which facilitates a good load transfer to the GA network [24,40,41].

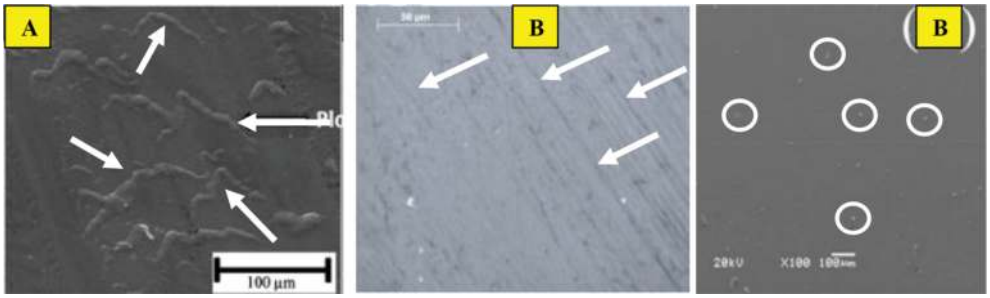

Figure 13. SEM images of worn surfaces of (A) CNF/UHMWPE, (B) CNT/UHMWPE, and (C) GA/UHMWPE.

2.5.6. Physical properties

2.5.6.1. Density

The density of UNC can be calculated with the Archimedes principle through weighing the sample in air and ethanol as an immersion medium using a high-sensitivity electronic weighing balance with accuracy (10^{-4} g). Previous studies showed that the density of UHMWPE remained the same, because the ratio of nanofiller to the volume of nanocomposite is very small and the densities of the nanofillers are very low [41].

2.5.6.2. Wettability

The wettability or contact angle (θ) of UNC can be evaluated using a high-resolution camera as shown in **Figure 14**. A 5 µl drop was deposited on the sample surface and θ can be measured after a few seconds. Any software, such as ImageJ, can be used to capture and analyze the contact angle. The results show that the contact angle increased with the addition of the nanofiller due to the modification of the surface and improvement of the surface roughness by adding nanofills [42].

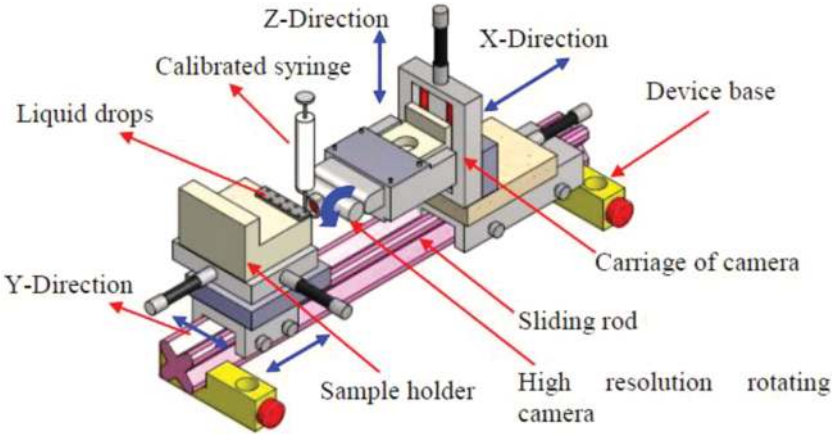

Figure 14. Schematics of contact angle device measurement.

2.5.7. Biocompatibility

Biocompatibility or cytotoxicity studies were conducted to show and evaluate the biocompatibility of the UNC. Ge et al. and Huang et al. studied the effect of adding ultralow molecular weight polyethylene and natural coral particles on the biocompatibility of UHMWPE [43,44]. The results showed that all cells are attached and spread, proliferate nicely, and grow in synthesis sheets. For carbon fillers, the studies reported GA more than CNT with a slight increase [45]. Therefore, the trend now is to use GA as a biocompatibility nanofiller.

2.5.8. Effect of UV radiation on wear resistance

It is supposed that replacement joints are exposed to the influence of some environmental factors during daily life. These factors should be taken into consideration during the design process to determine the extent of their impact on the performance and service life. Weather tester equipment is used for simulating sunlight with a light source of fluorescence. The experiment can be conducted according to the ASTM G154-06 standard. The samples were exposed to UV radiation for a period of 300 h at a temperature of 60°C without water condensation or spraying cycle. The results showed that UV radiation has no effect on the wear durability or any peeling off of the nanocomposite at the low number of cycles, with microvoids appearing with the increase in the number of cycles [46].

2.5.9. Degrading action

In general, AJ works in wet lubricant ambient environment to reduce the wear rate. Therefore, nature's lubricant might affect the degradation of UHMWPE, particularly mechanical and physical properties. In this section, the prepared samples (UHMWPE and its composites) are exposed to hyaluronic acid for different intervals (several months) and then studied for the

effects on the performance. Hyaluronic acid is a simulated synovial liquid. Most previous studies focused on pristine UHMWPE and modified UHMWPE. The results showed that the performance of pure UHMWPE decreased, whereas the modified one had a small change as a result of cross-linking that prevents their sliding in the presence of acid and thus increase the polymeric resistance to the degradation action [47]. Unfortunately, there are no previous studies focused on UHMWPE, except Yousef (under review). Regarding UHMWPE reinforced by carbon nanofiller, the results showed that nanocomposites are more stable.

2.6. Summary

CNT, GA, and CNF are considered the common nanomaterial types used to enhance UHMWPE using many methods for dispersion such as hot plate, magnetic stir bar, ultrasonic bath, ball milling, twin-screw extrusion, and three roll mill. The hot press is used to compress the UNC clay and then produce the sheets. The characterizations of the UNC sheets depend on the percentage weight of the nanofiller and dispersion technique. The previous results showed that the characterizations of UHMWPE improved by adding CNT and GA. Also, the studies reported the biocompatibility of GA/UHMWPE more than CNT/UHMWPE with a slight increase.

3. Nanocomposite polymer CNT/UHMWPE hip cup

This section presents a novel technique to produce a real polymer nanocomposite hip cup using paraffin oil dispersion technique, which has been innovated in the recent years by Yousef et al. [48]. In addition, the wear behavior of the hip can be investigated using an AJ simulator (AJS) built especially for this by Yousef et al. (under research).

3.1. Synthesis of nanocomposite polymer hip cup

Previous studies have focused on the production of UNC fit for use in biomaterial applications within the laboratory scale precisely for UNC thin sheets. These studies did not live up to the actual implementation due to the high viscosity, which is considered as the main obstacle in obtaining a regular dispersion during the mixing process even on the laboratory scale. This was the motivation for Yousef to innovate the paraffin oil dispersion technique to produce polymer nanocomposite bulk components. In this section, the new dispersion technique will be employed after making some modifications to produce the CNT/UHMWPE hip cup as explained in the following steps.

3.2. Materials

Three materials are used in this study for the synthesis of the real nanocomposite hip cup: UHMWPE as a base material, CNT as a nanofiller material, and paraffin liquid (PL) as an assist melt during the injection process.

3.3. Synthesis of CNT/UHMWPE short bars

First, UHMWPE and CNT (0.5–1% wt.) were mixed together using (a) hot plate or magnetic stir bar and (b) ultrasonic bath, ball milling, or three roll mill at different conditions to find the optimum dispersion method and conditions to obtain CNT/UHMWPE clay. With regard to the EX dispersion, it is not preferred in this case because it is more expensive. Second, the CNT/UHMWPE powder is mixed with PL (2% wt.) at 125°C using magnetic stirring bar for 5 to 10 to absorb PL. Third, the injection moulding die, which was designed and manufactured by Yousef et al., was used to synthesize short PNC bars with diameters of 45 mm and length of 80 mm (**Figure 15**). The following steps are followed in the production of the flanges and short bars:

- CNT/UHMWPE clay is poured into a hopper machine.
- An electric heater increases the mixing chamber temperature to 140°C.
- When 140°C is reached, a screw thread begins to rotate to push the melt powder along the heater.
- The liquid is injected into the molded die to form the short bar and then cooled to produce the final shape.

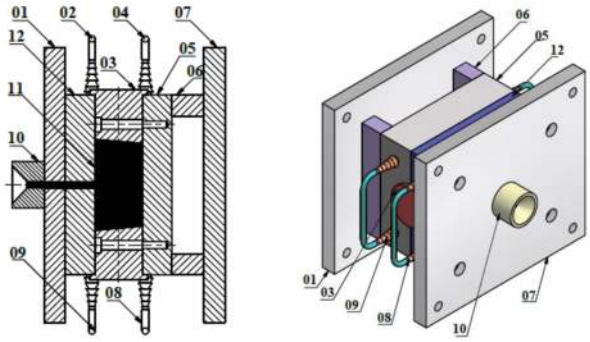

01) Supported movable die, 02-04) cooling water exit, 03) Movable die, 05) Supported fixed die, 06) Fixed die, 07) Injected flange, 08) Die support with extruder head, and 02-04) Cooling water inlet.

Figure 15. Schematic drawing of the short bar injection die [49,50,51].

3.4. Manufacturing of CNT/UHMWPE hip cup

The lathe machine was employed to machining the short bar to realize that the final shape of the hip cup has an inner diameter of 28 mm and thickness of 7 mm. In addition, external flange, which is used to fix the hip cup on the test rig, can be machined by the lathe also.

3.5. AJS design

This section presents a new approach to investigate the wear rate of CNT/UHMWPE hip cup. The new simulator has been designed to address some of the frailties of the other hip test rigs and to make it more flexible by controlling the following parameters: (i) dynamic weight value, (ii) length of leg and thigh, (iii) gait angle, (iv) linear velocity, and (v) dry or wet lubricant conditions. The idea of the new design depends on preventing the upper human body from moving in the front and back directions (X-direction) and allowing to move in the vertical direction (Y-direction) only to overcome the reaction that results during the collision of the foot with the ground (**Figure 16**). It is worth mentioning that the spring is used to generate the dynamic load during the testing process and the length of the vertical movement is equal to the spring deflection. Also, the stepper motor is used to rotate the quick-return mechanism and thus move the ground as an oscillatory motion in the X-direction. The oscillatory motion has been designed to simulate the real movements of the human body (reverse the reality; the ground is fixed and the human body is moveable) and thus decrease the simulator size. In addition, the oscillatory motion is responsible to rotate the leg link around the knee joint and then the resulting rotational motion transfer to the thigh arm to begin the contact between the

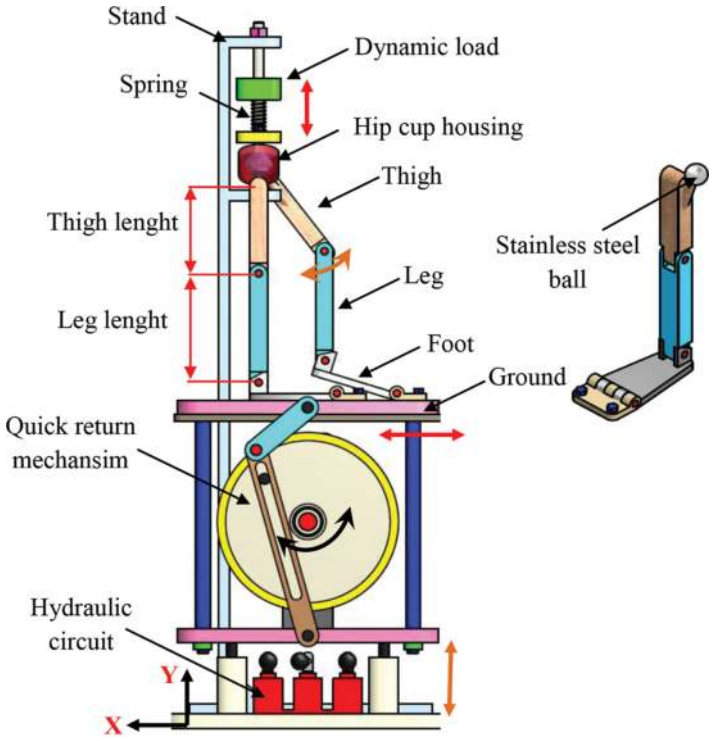

Figure 16. Joint Replacement Simulator.

metal and polymer components. Furthermore, loosening occurs and two types of wear failure mechanisms (sliding and rolling) appear. Finally, the simulator has the possibility to investigate the wear under dry and wet conditions by adding the lubricant inside the hip cup housing.

3.6. Wear hip cup investigation

The wear rate in the new design depends on six variables, such as the length of the femur, length of the tibia, gait angle, applied load, and metallic material (stainless steel or ceramic material), in addition to the lubricant conditions. To simulate the operating environment, usually the wear of the hip cup is investigated in dry or wet ambient environment. Most previous studies use distilled water or synovial fluid (SF) as a wet lubricant. SF can be defined as a natural lubricant and considered as the standard lubricant of these applications, because SF consists of many biological molecules such as proteins, lipids, and polysaccharides leading to improve the surface properties [51]. Distilled water is used as a simulated lubricant due to it being more abundant compared to SF. Furthermore, it is difficult to take all the previous variables into account during the testing process, but there are priorities that can be chosen depending on the human age and environmental effects. The wear behavior in this case can be evaluated by the weight or volume loss (in the form of mass loss) by weighing the tested hip cup on a high-sensitivity balance with high accuracy (10^{-4} g) after and before every test. The test can be repeated many times to determine the optimal percentage weight ratio of the CNT in the UHMWPE matrix. To investigate the effect of CNT added on the wear mechanism of the UHMWPE hip cup, optical microscopy is recommended to examine the worn surfaces. Finally, it is expected that these variables will affect the service life and give the most accurate values. Also, wear resistance will increase with the addition of CNT using the new dispersion technique and obstruct wear progress due to the following causes:

- The addition of paraffin oil during the injection process to UHMWPE led to a decrease in viscosity and then resulted in a good mixing (dispersed) with the CNT.
- Paraffin oil can be used also in this case as a lubricating oil. Similarly, CNT is used as a solid lubricant even in the event of agglomeration.
- Previous studies showed that the melting temperature of UHMWPE grows when mixed with the CNT. This process leads to the destruction of the surface layer because thermally softening occurs early, thus, decreasing the wear rate.

4. Conclusion

In this chapter, the author reviewed an overview of the AJ, including its components, most common polymeric materials used for these applications, reasons of failures, and characterization methods. Then, the author touched the methods of improving the performance of polymeric materials through mixing it with several types of nanofiller materials using many methods of dispersion. The chapter overview is focused on UHMWPE as a polymer base and CNT as a nanofiller. In addition, some nanofiller materials such as GA and CNF are pre-

sented also for comparison. The author presented a novel technique to produce a real UNC hip cup that has high wear resistance using the paraffin oil dispersion technique. Finally, to investigate the wear behavior of the new cup, AJS has been designed to be comparable to the human body movement approximately to increase the accuracy of the results. Finally, regarding the advantages of the polymer nanocomposite AJ compared to the traditional AJ, the wear resistance of the new joints will increase and thus increase the service life. The side effect summarized in the traditional AJ has biocompatibility slightly better than the nanocomposite.

Author details

Samy Yousef

Address all correspondence to: ahcann@hotmail.com

Department of Production Engineering and Printing Technology, Akhbar Elyom Academy, Giza, Egypt

References

[1] http://www.clipartof.com/portfolio/pmrk/illustration/3d-human-male-skeleton-sitting-and-thinking-1073684.html.

[2] http://www.niams.nih.gov/health_info/joint_replacement/#2.

[3] Charnley J. Arthroplasty of the hip. A new operation. Lancet 1 (1961) 1129–1132.

[4] http://www.hipandpelvis.com/for-patients/patient-education/patient-education-anterior-approach-tha/.

[5] Brems J. The glenoid component in total shoulder arthroplasty. J. Shoulder Elbow Surg. 2 (1993) 47–54.

[6] https://www.hss.edu/conditions_arthritis-of-the-knee-total-knee-replacement.asp.

[7] http://www.arthritiscentre.org/for-the-professional/services-for-gps-other-professionals/upper-limb-surgery-clinic/.

[8] Bistolfi A., Bellare A.. The relative effects of radiation crosslinking and type of counterface on the wear resistance of ultrahigh-molecular-weight polyethylene. Acta Biomater. 7 (2011) 3398–3403.

[9] Lu S., Liang G., Zhou Z., Li F.. Structure and properties of UHMWPE fiber/carbon fiber hybrid composites. J. Appl. Polym. Sci. 101 (2006) 1880–1884.

[10] Baena J.C., Wu J., Peng Z. Wear performance of UHMWPE and reinforced UHMWPE composites in arthroplasty applications: a review. Lubricants 3 (2015) 413-436.

[11] Hulbert S.F., Megremis S.J.. Effects of UHMWPE wear debris generated from total hip and total knee replacements. 1996 IEEE 0-7803-3 13 1.

[12] Valenza A., Visco A.M., Torrisi L., Campo N.. Characterization of ultra-high-molecular-weight polyethylene (UHMWPE) modified by ion implantation. Polymer 45 (2004) 1707–1715.

[13] Xue Y., Wu W., Jacobs O., Schädel B.. Tribological behaviour of UHMWPE/HDPE blends reinforced with multi-wall carbon nanotubes. Polym. Test. 25 (2006) 221–229.

[14] Saikko V., Shen M.. Wear comparison between a dual mobility total hip prosthesis and a typical modular design using a hip joint simulator. Wear 268 (2010) 617–621.

[15] Geary C., G.E. O'Donnell, Jones E., FitzPatrick D., Birkinshaw C.. Automated in-vitro testing of orthopaedic implants: a case study in shoulder joint replacement. Proc. Inst Mech Eng Vol. 224 Part H: J. Eng. Med.

[16] Saikko V., Ahlroos T., Calonius O.. A three-axis knee wear simulator with ball-on-flat contact. Wear 249 (2001) 310–315.

[17] Bascarevic Z., Vukasinovic Z., Slavkovic N., Dulic B., Trajkovic G., Bascarevic V., Timotijevic S.. Alumina-on-alumina ceramic versus metal-on-highly cross-linked polyethylene bearings in total hip arthroplasty: a comparative study. Int. Orthopaed. (SICOT) 34 (2010) 1129–1135.

[18] van der Pijl A.J., S´wiszkowski W., Bersee H.E.N.. Design of a wear simulator for in vitro shoulder prostheses testing. Technical Application Series, 2004.

[19] Rodriguez J.A. Cross-linked polyethylene in total knee arthroplasty. J. Arthroplast. 23 (2008).

[20] Joyce T.J., Unsworth A.. The design of a finger wear simulator and preliminary results. Proc. Inst. Mech. Eng. Vol. 214 Part H. S. Yousef. Polymer Nanocomposite Components: A Case Study on Gears (Woodhead, Cambridge, in press).

[21] Wannasri S., Panin S.V., Ivanova L.R., Kornienko L.A., Piriyayon S.. Increasing wear resistance of UHMWPE by mechanical activation and chemical modification combined with addition of nanofibers. Procedia Eng. 01 (2009) 67–70.

[22] Maksimkin A.V., Kaloshkin S.D., Kaloshkina M.S., Gorshenkov M.V., Tcherdyntsev V.V., Ergin K.S., Shchetinin I.V.. Ultra-high molecular weight polyethylene reinforced with multi-walled carbon nanotubes: fabrication method and properties. J Alloy Compd. 536 (2012) S538–S540.

[23] Lahiri D., Hec F., Thiesse M., Durygind A., Zhang C., Agarwal A.. Nanotribological behavior of graphene nanoplatelet reinforced ultra high molecular weight polyethylene composites. Tribol. Int. 70 (2014) 165–169.

[24] Wood W.J., Maguire R.G., Zhong W.H.. Improved wear and mechanical properties of UHMWPE-carbon nanofiber composites through an optimized paraffin-assisted melt-mixing process. Composites Pt. B 42 (2011) 584–591.

[25] Kanagaraj S., Mathew M.T., Fonseca A., Oliveira M.S.A., Simoes J.A.O., Rocha L.A., L.A. Tribological characterisation of carbon nanotubes/ultrahigh molecular weight polyethylene composites: the effect of sliding distance. Int. J. Surf. Sci. Eng. 4 (2010) 305–321.

[26] http://www.imatproject.eu/en/technology-111/carbon-nanotubes-124.

[27] Yousef S., Khattab A., Osman T.A., Zaki M.. Fully automatic system for producing carbon nanotubes (CNTs) by using arc-discharge technique multi electrodes. ICIES (2012).

[28] Yousef S., Khattab A., Osman T.A., Zak M.. Effects of increasing electrodes on CNTs yield synthesized by using arc-discharge technique. J. Nanomater. 2013 (2013) 392126.

[29] Mohamed A, Yousef S.. CNT mass production by using CVD multi quartz tubes.

[30] Eklund P.C., Pradhan B.K., Kim U.J., Xiong Q.. Large-scale production of single-walled carbon nanotubes using ultrafast pulses from a free electron laser. Nano Lett. 2 (2002) 561–566.

[31] Visco A.M., Yousef S., Galtieri G., Nocita D., Pistone A., Njuguna J.. Thermal, Mechanical and Rheological Behaviors of Nanocomposites Based on UHMWPE/Paraffin Oil/Carbon Nanofiller Obtained by Using Different Dispersion Techniques. JOM-Springer 2015. DOI 10.1007/s11837-016-1845-x

[32] Yousef S., Visco A., Galtieri G., Nocita D.. Improved wear resistance of UHMWPE based nanocomposites for prosthetic applications, filled with liquid paraffin and carbon nanofibers. INSTM Conf. Italy (2015).

[33] Golchin A., Wikner A., Emami N.. An investigation into tribological behaviour of multi-walled carbon nanotube/graphene oxide reinforced UHMWPE in water lubricated contacts. Tribol. Int. 95 (2016) 156–161.

[34] Zuo J., Zhu Y., Liu S., Jiang Z., Zhao J.. Preparation of HDPE/UHMWPE/MMWPE blends by two-step processing way and properties of blown films. Polym. Bull. 58 (2007) 711–722.

[35] Yousef S., Visco A.M., Galtieri G., Njuguna J.. Wear characterizations of polyoxymethylene (POM) reinforced with carbon nanotubes (POM/CNTs) using the paraffin oil dispersion technique. JOM-Springer 2015. DOI: 10.1007/s11837-015-1674-3.

[36] Ruan S.L., Gao P., Yang X.G., Yu T.X.. Toughening high performance ultrahigh molecular weight polyethylene using multiwalled carbon nanotubes. Polymer 44 (2003) 5643–5654.

[37] Ma H., Chen X., Hsiao B.S., Chu B.. Improving toughness of ultra-high molecular weight polyethylene with ionic liquid modified carbon nanofiber. Polymer 55 (2014) 160–165.

[38] Chen Y., Zou H., Liang M., Liu P.. Rheological, thermal, and morphological properties of low-density polyethylene/ultra-high-molecular-weight polyethylene and linear low-density polyethylene/ultra-high-molecular-weight polyethylene blends. J. Appl. Polym. Sci. 2013. DOI: 10.1002/APP.38374.

[39] Kumar R.M., Sharma S.K., Kumar B.V.M., Lahiri D.. Effects of carbon nanotube aspect ratio on strengthening and tribological behaviour of ultra high molecular weight polyethylene. Composite 76 (2015) 62–72.

[40] Liu Y., Sinha S.K.. Wear performances and wear mechanism study of bulk UHMWPE composites with nacre and CNT fillers and PFPE overcoat. Wear 300 (2013) 44–54.

[41] Tai Z., Chen Y., An Y., Yan X., Xue Q.. Tribological behavior of UHMWPE reinforced with graphene oxide nanosheets. Tribol. Lett. 46 (2012) 55–63.

[42] Yousef S., Visco A.M., Galtieri G., Njuguna J.. Flexural, Impact, Rheological and physical Characterizations of POM Reinforced by Carbon Nanotubes and Paraffin Oil. Polymers for Advanced Technologies. (In press)

[43] Huang Y.-F., Xu J.-Z., Li J.-S., He B.-X., Xu L., Li Z.-M.. Mechanical properties and biocompatibility of melt processed, self-reinforced ultrahigh molecular weight polyethylene. Biomaterials xxx (2014) 1–11.

[44] Ge S., Wang S., Huang X.. Increasing the wear resistance of UHMWPE acetabular cups by adding natural biocompatible particles. Wear 267 (2009) 770–776.

[45] Chen Y., Qi Y., Tai Z., Yan X., Zhu F., Xue Q.. Preparation, mechanical properties and biocompatibility of graphene oxide/ultrahigh molecular weight polyethylene composites. Eur. Polym. J. 48 (2012) 1026–1033.

[46] Abdul Samad M., Sinha S.K.. Effects of counterface material and UV radiation on the tribological performance of a UHMWPE/CNT nanocomposite coating on steel substrates. Wear 271 (2011) 2759– 2765.

[47] Visco A.M., Campo N., Torrisi L., Cristani M., Trombetta D., Saija A.. Electron beam irradiated UHMWPE: degrading action of air and hyaluronic acid. Bio-Med. Mater. Eng. 18 (2008) 137–148.

[48] Yousef S., Khattab A., Zak M., Osman T.A.. Wear characterization of carbon nanotubes reinforced polymer gears. IEEE Trans. Nanotechnol. 12 (2013) 616–620.

[49] Yousef S., Osman T.A., Khattab M., Bahr A.A., Youssef A.M.. A new design of the universal test rig to measure the wear characterizations of polymer acetal gears (spur, helical, bevel, and worm). Adv. Tribol. DOI: org/10.1155/2015/926918.

[50] Yousef S., Osman T.A., Abdalla A.H., Zohdy G.A.. Wear characterization of carbon nanotubes reinforced acetal spur, helical, bevel and worm gears using a TS universal test rig. JOM-Springer, DOI: 10.1007/s11837-014-1268-5.

[51] Yousef S. Chapter 16: Polymer nanocomposite components: a case study on gears. Elsevier, 2016. Lightweight Composite Structures in Transport,. ISBN: 978-1-78242-325-6. http://dx.doi.org/10.1016/B978-1-78242-325-6.00016-5

[52] Kung M.S., Markantonis J., Nelson S.D., Campbell P.. The synovial lining and synovial fluid properties after joint arthroplasty. Lubricants 3 (2015) 394–412. DOI: 10.3390/lubricants3020394.